Colloid and Interface Science Communications 16 (2017) 25–29

Contents lists available at ScienceDirect

Colloid and Interface Science Communications

journal homepage: www.elsevier.com/locate/colcom

Rapid Communication

Optical Detection of Nanoaggregates in highly Concentrated strongly Absorbing Colloids without Sample Dilution

S. Bali [a,*], J.T. Boivin [b], R.N.M. Ducay [a], N. Phillip [a], J.D. Brinton [a], L.M. Bali [a], J.P. Scaffidi [c], J.A. Berberich [b,*]

[a] Department of Physics, Miami University, Oxford, OH 45056, United States
[b] Department of Chemical, Paper and Biomedical Engineering, Miami University, Oxford, OH 45056, United States
[c] Scaffidi Scientific Consulting, Philadelphia, PA 19144, United States

ARTICLE INFO

Article history:
Received 1 September 2016
Received in revised form 22 December 2016
Accepted 19 January 2017
Available online xxxx

Keywords:
Nanoparticle
Refractometer
Aggregation
Total internal reflection
Optical sensor
Turbid media

ABSTRACT

The ability to monitor the flocculation, aggregation and settling of micro and nano-sized particles is important for many environmental, chemical, biological and biomedical processes. However, standard approaches such as dynamic light scattering or absorption spectroscopy require sample dilution for characterization of highly concentrated samples. In this model study a new method using total internal reflection (TIR) is demonstrated to directly detect aggregates in highly-concentrated, strongly-absorbing samples of aqueous gold nanoparticles without sample dilution or pretreatment. Aggregation of the gold nanoparticles is induced by changing solution pH or by increasing ionic strength. Results obtained using the new sensor with no dilution agree with the post-dilution results obtained by absorption spectroscopy, dynamic light scattering, and zeta potential measurements. This validation of the sensor by standard methodologies is important because earlier work with sensitive detection of aggregates in non-absorbing polystyrene nanoparticles precluded the use of standard methodologies.

Detecting the flocculation, aggregation and settling of micro and nanoparticles is important for many environmental [1], biological and biomedical processes [2,3]. In many applications, it is important to monitor in-situ and in real-time the synthesis, settling or aggregation of nanoparticles [4–6]. Scattering-based methods such as Dynamic Light Scattering (DLS) and zeta potential measurement provide a measure of particle size, particle dispersity, and surface charge. DLS relies on a correlation measurement of scattered photons and is regarded as the gold standard in such applications, compared to simple scattering intensity measurements (turbidimetry) or transmission intensity measurements (nephelometry). However, the single-scattering assumption needs to be satisfied in all these approaches, requiring significant sample dilution in the case of concentrated or highly turbid samples in order to avoid multiple scattering artifacts. Also, DLS and zeta potential measurement are suited only for particles in a narrow size range at commonly used visible wavelengths and typically fail for particle sizes exceeding a micron.

The above scattering-based methods are whenever possible complemented by transmission-based methods such as absorption spectroscopy at UV–visible frequencies (UV–Vis) which is often used to monitor particle aggregation, flocculation and settling for weakly absorbing colloids such as TiO_2, ZnO, and biological cells. However, only a narrow concentration range can be used in UV–Vis methods since the absorbance remains linear up to a value of approximately 2. Highly absorbing gold nanoparticles require significant dilution in order to satisfy the single-scattering assumption.

Note that the above discussion pertains to optical detection methods. Recently, non-optical acoustoelectric methods have been developed that are capable of particle-sizing in highly concentrated dispersions, provided a density difference exists between the suspended particle and the medium [7]. On the other hand, optical methods rely on a difference in refractive index, hence offering a viable alternative in cases where the density difference is small. For example, in aqueous suspensions of polystyrene microspheres the density difference is just a few percent but the refractive index difference is nearly 20%. Thus, optical and acoustoelectric particle-sizing methods are complementary and are well worth developing side-by-side.

In colloids, the scattering particle size is comparable to the optical wavelength. A useful optical parameter for quantifying the colloid concentration is the attenuation coefficient (α in cm^{-1}) which is defined through Beer's Law: the intensity $I(z)$ of a light beam propagating in the z-direction through the colloid attenuates owing to scattering and/or absorption and is given by $I(z) = I_0 e^{-\alpha z}$, where I_0 is the intensity at $z = 0$. In the context of highly dense colloids ($\alpha > 200\ cm^{-1}$), it has been pointed out that total internal reflection (TIR) based imaging methods offer important unique advantages [8,9]. *In TIR, the sample penetration lengths are only on the order of an optical wavelength, meaning the single-scattering assumption is satisfied despite the high particle density in undiluted samples* - for visible wavelengths this assumption breaks

* Corresponding authors.
E-mail addresses: balis@miamioh.edu (S. Bali), berberj@miamioh.edu (J.A. Berberich).

http://dx.doi.org/10.1016/j.colcom.2017.01.001

down only at extremely high attenuations on the order of 10^4/cm [9,10]. Among TIR-imaging methods some of the most widely used state-of-the-art techniques are based on surface plasmon resonance (SPR) in a metal film, usually gold, deposited on a glass surface. In this approach, the sample to be analyzed is placed on top of the gold-coated glass surface and the angle or wavelength of the incident light is varied. However, the chemical inertness that makes gold a practical choice in SPR sensors also makes gold a difficult substrate to adsorb to [11]. Some biological molecules do adsorb, only to denature in contact with the metal [12]. On the other hand, it has been pointed out that gold-thiol-dextran functionalization chemistry, which is the cornerstone for SPR, does not apply to surface science investigation in the vast microelectronics industry where organic functionalization on silica is required [13] - silane-based chemistries are preferred to gold-thiol-based in this case [14]. It is therefore desirable to consider TIR-based methods that do not suffer from this important limitation of SPR.

In this short communication we show that, by tracking the attenuation coefficient α, it is possible to directly monitor aggregation of highly dense aqueous colloidal gold nanoparticles (AuNPs) without sample dilution or pretreatment using a novel TIR-based sensor which does not require a gold film - the sample is placed directly on an uncoated glass surface – hence the sensor is free from the limitations of SPR discussed above. The densities used are comparable to the densest aqueous gold colloids reported in the literature [15]. Aggregation is induced either by changing the solution pH or the ionic strength and it is shown that the α-measurement can be used as a direct and sensitive marker for distinguishing between aggregated and non-aggregated AuNP suspensions. Furthermore, particle aggregation is monitored by UV–Vis spectroscopy, zeta potential measurement, and DLS, and close agreement is obtained with TIR measurements. The ability to corroborate results from the sensor with standard methods is a significant advantage over recent similar work performed in highly scattering suspensions of non-absorbing polystyrene nanospheres [8]. In Ref. [8], the absence of plasmonic absorption and scattering precluded the use of UV–Vis, and DLS was shown to be ineffective. Furthermore, since zeta potential is just derived from a DLS measurement under an applied electric field, no systematic experimental corroboration of our TIR-based sensor existed until this communication. The results presented here and in Ref. [8] demonstrate that the TIR-based sensor can detect nanoaggregation in optically dense plasmonic and non-plasmonic particulate suspensions.

Gold nanoparticles (AuNPs) were prepared by the Lee-Meisel citrate reduction procedure [16], and carboxylic acid functionality was provided by adding mercaptopropionic acid (MPA) – see Supplementary information Sec. S-I. The negative charges from the propionic acid stabilize particles against van der Waal's attraction and prevent aggregation. The Au concentration in the MPA-functionalized AuNP solutions was determined to be 27 parts per thousand (mg/mL) by ICP-MS. DLS measurements indicated a hydrodynamic diameter of 95 nm after functionalization with MPA, giving a particle concentration of ~3.0×10^{10} AuNPs/mL.

Aggregation was induced by adding 2.2 mL of either HCl to change the pH or NaCl to increase the ionic strength, to 800 μL of the functionalized AuNP solution. The final samples contained ~8.0×10^9 AuNPs/mL with varying concentrations (0.1 mM to 50 mM) of HCl or NaCl.

The sensor geometry is based on a glass prism in the standard Kretschmann configuration often used in SPR, and has been described in detail earlier [8–10,17–19]. The only difference with previous setups is that in the present work a glass coverslip is inserted above the BK7 glass prism, and the dense colloidal sample is placed on top of the coverslip, as shown in Fig. 1 (a). This is necessary when working with Au NP colloidal samples since it was found to be especially difficult to completely clean off the glass prism surface within a practical timeframe [20]. Refractive index matching fluid is used between the coverslip and the prism, and the coverslip is allowed to settle for 15 min before sample placement.

The colloidal sample is illuminated by a spatially divergent p-polarized beam of intensity I_i (typically 6 μW) from a laser diode of center wavelength 653 nm with a bandwidth of ±4.5 nm. The diode is pigtailed to a single mode fiber to produce a pure Gaussian spatial profile. The light reflected from the cover slip-sample interface, denoted by I_r, is allowed to fall on a one-dimensional uncooled pixel array (Perkin-Elmer, Model no. LD3522PGK-022, 1024 pixels, each of width 14 μm), and the intensity in each pixel is read out in near real-time using a LabVIEW program. The sample volume is ~0.3 mL, sufficient to cover the laser spot size (~3–4 mm) at the prism-sample interface. The range of angles θ_i incident on the prism-sample interface that are detected by the pixel array spans both TIR and non-TIR regions, yielding reflectance profiles as shown by the two solid curves in Fig. 1(b) - the top (gray) curve is for an aqueous gold nanoparticle suspension in which no aggregates exist, clearly distinct from the lower (blue) curve which is for the same suspension in which aggregation has been induced by adding HCl to reduce the solution pH. See Supplementary information Sec. S-III for details on how the reflectance profiles in Fig. 1(b) are generated. Details of sensor calibration, and an analysis of the sources of error in our sensor, are provided in Ref. [19].

The dashed lines (red) in Fig. 1 (b) are theoretical fits derived from Fresnel theory, but the theory is modified to correctly account for the loss in TIR intensity owing to scattering/absorption of the evanescent wave as it penetrates into the colloidal medium. Details of the modified Fresnel model are presented in Refs. [8–10,17–19]. In short, the fit consists of the usual Fresnel reflectance formula for I_r / I_i (θ_i), which is a

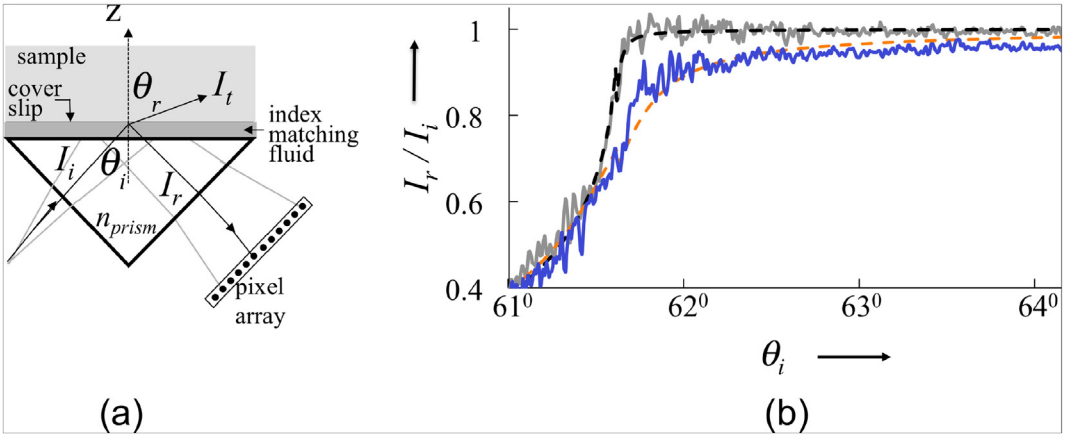

Fig. 1. (a) Prism-sample interface with glass cover slip and index-matching fluid of refractive index 1.5167 ± 0.0005. Gravity points in the $-z$ direction. (b) Typical plot of experimental reflectance profile I_r / I_i (θ_i) for non-aggregated (gray curve, top) and aggregated (blue curve, bottom) dense Au NP suspensions. The dashed lines are theoretical fits. (For interpretation of the references to color in this figure legend, the reader is referred to the web version of this article.)

function of not just θ_i but also the real and imaginary parts of the colloidal refractive index n_r and n_i [21]. In standard Fresnel theory n_i is a constant for all angles of incidence, but in the modified theory n_i is taken to be angle-dependent for those incident angles where TIR exists. We write $n_i(\theta_i) = a\,\kappa(\theta_i)$ where $\kappa(\theta_i)$ is the ratio of the evanescent wave's penetration depth to the optical wavelength, and a is the value of the imaginary refractive index for perpendicular incidence, which is related to the attenuation coefficient α through the relation $\alpha = 2a\omega/c$ (where $\omega/2\pi$ is the laser frequency and c is the speed of light). As explained in detail in Refs. [8–10,17–19], a theoretical best-fit to each reflectance data-profile is constructed by varying the two fitting parameters n_r and n_i so as to minimize the mean-square deviation between the data and the modified Fresnel reflectance formula.

It is important to note that upon the addition of an aggregation-inducing agent, the aggregation kinetics in highly concentrated Au or Ag colloids are, just as in the case of non-plasmonic polystyrene nanospheres [8], too fast to be detected directly by the sensor. However, when the aggregated sample is placed on top of the TIR sensor, the aggregates slowly settle and are sensed as they approach within a wavelength of the glass-sample interface, causing an increase in the attenuation coefficient measured by the sensor. Fig. 2 shows measurements of the attenuation coefficient α as a function of time. Starting from 30 s after the aggregated sample was deposited on the cover slip, α- measurements were made at one-minute intervals for a total of 30 min, indicating that settling of the AuNP aggregates occurs on the time-scale of few tens of minutes.

Fig. 2 confirms that the sensor detects settling due to aggregation and not due to any other cause, and also establishes the time-scale for settling. First, $\alpha(t)$ was measured for a suspension of carboxylated AuNPs in deionized water when mixed with 350 mM HCl (blue solid triangles). Next, the sample was cleaned off the sensor, and an identical aqueous sample of AuNPs mixed with HCl was prepared but this time 15 min was waited, a time much longer than that required for any aggregation processes to possibly occur, before placing the sample on the sensor and initiating measurement of $\alpha(t)$ (white squares). Both samples yield nearly identical $\alpha(t)$ - curves, with α rising from 10 cm^{-1} to ~1000 cm^{-1} over a period of 15 min. This clearly indicates that the sensor detects settling onto the prism- coverslip interface which initiates as soon as the sample is placed on the sensor. Finally, to confirm that it is indeed only aggregates that are settling, α was measured as a function of time for an identical aqueous sample of AuNPs, but this time without adding any HCl (Orange squares). No significant settling occurs in the absence of aggregate formation [22].

Based on Fig. 2 in which we see the α-value beginning to level off at the 15 min mark, we empirically pick 30 min as the time at which we deem that the settling process is, for the most part, over - thus achieving the maximum sensitivity achievable by the sensor which is based on detecting aggregation via settling. At this time the difference in α-value between the aggregated and unaggregated samples is about 100:1.

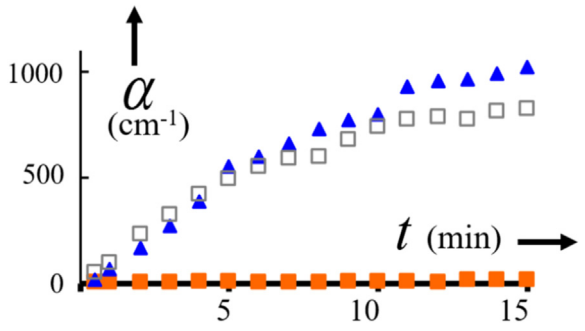

Fig. 2. Measurement of settling time for aggregated (blue triangles and white squares) and non-aggregated (orange squares) AuNPs. (For interpretation of the references to color in this figure legend, the reader is referred to the web version of this article.)

Each reflectance profile in Fig. 1(b) was recorded after the sample was allowed to sit on the prism for 30 min. If, on the other hand, one deems a signal of 40:1 as sufficient to detect the presence of aggregation, Fig. 2 shows that one may plot reflectance data after letting the sample sit on the prism for only about 4 min.

In Fig. 3 the data for detection of aggregation in dense AuNP colloidal solutions is plotted using three different methods, our TIR sensor, UV–Vis absorption spectroscopy, and DLS, and show that these methods yield results that are consistent with each other. Each of the three plots on the left in Fig. 3(a) indicates that pH-induced aggregation occurs at an HCl concentration > 0.2 mM (pH < 3.7). On the right, each of the three plots on the right in Fig. 3(b) indicates that aggregation induced by change in ionic strength occurs at an NaCl concentration between 30 and 40 mM. Zeta potential measurements are provided in the Supplementary information Sec. S-IV and indicate that aggregation begins to occur as zeta potential of the particles approaches zero. In order to perform the zeta potential and DLS measurements, significant sample dilution was required.

For these HCl and NaCl concentrations the top plots in Fig. 3(a) and (b) show a sharp increase in attenuation coefficient α caused by significant aggregate-settling as the sample is allowed to sit on our TIR sensor for 30 min. For an HCl (NaCl) concentration of 0.2 mM (20 mM) or below, minimal settling is observed, yielding an α-value that remains steady, between 10 and 60 cm^{-1}. The original gold nanoparticles were thoroughly tip sonicated before any aggregation measurements were made. Error bars for three data points are shown in the top plots in Figs. 3(a) and (b). The error bars for these three data-points are representative for other data-points in their vicinity.

No sample dilution was required for the UV–Vis analysis shown in Fig. 3. However, the α-values on the spectrophotometry plots in Fig. 3 are 2 orders of magnitude less than corresponding α-values obtained by the TIR sensor. This is because the same settling over time that causes aggregates to settle onto the sensor prism (thereby yielding α's of a few hundred cm^{-1}, see Fig. 2), also causes the aggregates to sink to the bottom of the cuvette employed in the spectrophotometer, meaning most of the aggregates have now fallen away from the center of the cuvette where the UV–Vis absorbance is measured (thereby yielding α's of only a few cm^{-1}). See Supplementary information Sec. S-V for a test of this assertion. Note that this effective dilution of the sample due to particles leaving the central sensing region of the cuvette is essential for recording UV–Vis absorption spectra since the spectrophotometer cannot measure absorbances exceeding 1.2 (i.e., α of 2.8) [22,23].

The aggregation of AuNPs leads to a color change from reddish-purple to bluish-purple (when viewed in transmission) due to the appearance of the surface plasmon bands which leads to a visible change in the optical properties of the colloid. The change in optical properties of the NP suspensions was monitored by measuring the UV–visible absorbance spectra (which was converted to α [23]) with increasing concentration of HCl or NaCl (Fig. 3). The unaggregated MPA-functionalized NPs have a surface plasmon band at 573 nm (this absorption in the green causes the solution to appear reddish-purple when viewed in transmission). Aggregation causes the surface plasmon band to red-shift and reduce in intensity due to the heterogeneous population of particle aggregates of different sizes. It is clear from the UV–Vis plots in Fig. 3 that the peak of the surface plasmon band shifts to ~710 nm for the aggregated AuNP solutions (this absorption in the red causes the solution to appear bluish-purple when viewed in transmission).

The concentrations of HCl and NaCl that result in a red-shift in the surface plasmon band match very well with the concentrations measured by the TIR sensor at which the sharp increase in attenuation α is recorded. These concentrations of HCl and NaCl at which the onset of aggregation occurs according to the TIR sensor and UV–Vis spectrophotometer are in agreement with zeta potential measurements (Fig. S1) that show a progressive reduction of zeta potential magnitude. Attractive Van der Waal's forces dominate over repulsive electrostatic forces at low zeta potential magnitude, enabling rapid aggregation – see

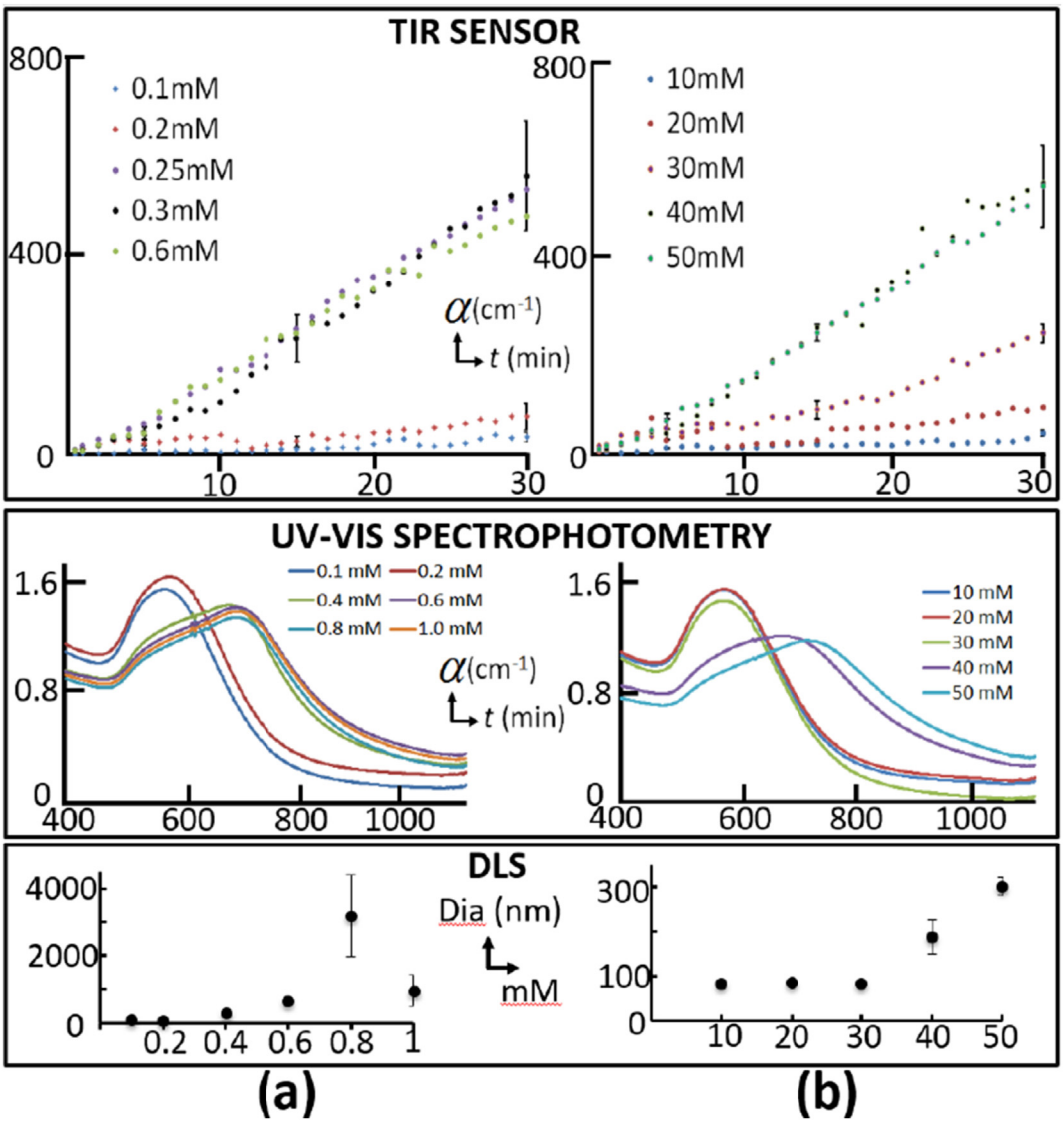

Fig. 3. Aggregation in AuNP suspensions due to change in a) pH, by adding HCl, or (b) ionic strength, by adding NaCl, as measured by three different methods. From top to bottom, we see that the onset of aggregation leads to a sharp increase in the attenuation coefficient α in our TIR sensor, a shift in peak absorbance in UV–Vis absorption spectroscopy (we convert absorbance to α [22] for convenient comparison with our sensor) and an increase in particle diameter measured by DLS. The TIR sensor (top) indicates that the onset of aggregation occurs at an HCl concentration > 0.2 mM (pH < 3.7) and an NaCl concentration between 30 and 40 mM, which is corroborated by the other methods.

Supplementary information Sec. S-IV for further explanation. Fig. 3 also shows that DLS measurements record a significant increase in NP-size from the original ~95 nm at 0.4 mM HCl and 40 mM NaCl, thus supporting the measurements from the TIR sensor, UV–Vis, and zeta potential.

In conclusion, we have demonstrated an optical method for rapid detection, without the need for any dilution or sample pretreatment, of the presence of aggregates in highly concentrated strongly-absorbing AuNP suspensions with densities comparable to the densest gold colloids reported in the literature. Note that the nearly isosbestic point in Fig. 3 at the operating wavelength of our sensor (653 nm) implies that, as desired, the sensor is sensitive only to the settling caused by aggregation, not so much to changes in absorbance caused by aggregation. Recently we demonstrated the success of this sensing method in highly scattering non-plasmonic suspensions [8] with polystyrene mass densities that were two orders of magnitude higher than previously reported – however, *in that work, we had no existing standard methods to check the validity of our results*, because the use of non-plasmonic particles precluded UV–Vis, and DLS (hence also zeta potential) was shown to be insensitive to the presence of small amounts of aggregates [8,24]. Here, working with plasmonic nanoparticles, we have obtained confirmation of the sensor's findings on aggregation with UV–Vis spectrophotometry, DLS and zeta potential measurement. This means that we now have experimental confirmation that the sensor may be used to accurately detect the presence of nanoaggregates in both plasmonic and non-plasmonic colloidal suspensions. As a potential future application, we note that the measurement of the attenuation coefficient α by our sensor may enable particle sizing [9], which is a topic of current interest specifically with regard to aggregate formation for chemical and biological sensing [25]. A current limitation of the TIR sensor is that the concentration must be confined to a regime where α stays a single-valued function of the particle size [8], and even when this condition is satisfied we can only extract an effective mean particle size, not a size distribution as is allowed by DLS [9].

Acknowledgments

We thank Miami University's Instrumentation Lab for providing assistance with the Labview code. Funding for this research was provided by Miami University's Interdisciplinary Roundtable Fund.

Appendix A. Supplementary Data

Supplementary data to this article can be found online at http://dx.doi.org/10.1016/j.colcom.2017.01.001.

References

[1] E.M. Hotze, T. Phenrat, G.V. Lowry, Nanoparticle aggregation: challenges to understanding transport and reactivity in the environment, J. Environ. Qual. 39 (2010) 1909–1924.
[2] A.E. Gregory, R. Titball, D. Williamson, Vaccine delivery using nanoparticles, Front. Cell. Infect. Microbiol. 3 (13) (2013) 1–13.
[3] W. Wang, Protein aggregation and its inhibition in biopharmaceutics, Int. J. Pharm. 289 (2005) 1–30.
[4] M. Collado-Gonzalez, V. Espin, M. Montalban, R. Pamies, J. Cifre, G. Banos, G. Villora, J. de la Torre, Aggregation behavior of gold nanoparticles in presence of chitosan, J. Nanopart. Res. 17 (268) (2015) 267–276.
[5] B. Abecassis, C. Bouet, C. Garnero, D. Constantin, N. Lequeux, S. Ithurria, B. Dubertret, B.R. Pauw, D. Pontoni, Real-time in situ probing of high-temperature quantum dots solution synthesis, Nano Lett. 15 (4) (2015) 2620–2626.
[6] T.J. Woehl, C. Park, J.E. Evants, I. Arslan, W.D. Ristenpart, N.D. Browning, Direct observation of aggregative nanoparticle growth: kinetic modeling of the size distribution and growth rate, Nano Lett. 14 (1) (2014) 373–378.
[7] See, for example. A.S. Dukhin, P.J. Goetz, Characterization of Liquids, Nano-and Microparticulates, and Porous Bodies using Ultrasound, second ed. Elsevier, 2010.
[8] J. Berberich, J. Scaffidi, R. Ducay, N. Phillip, J. Boivin, P. Judge, L. Bali, S. Bali, Direct detection of aggregates in highly turbid colloidal suspensions of polystyrene nanoparticles, Appl. Opt. 54 (21) (2015) 6461–6470.
[9] K. Goyal, M. Dong, V. Nguemaha, B. Worth, P. Judge, W. Calhoun, L. Bali, S. Bali, Empirical model of total internal reflection from highly turbid media, Opt. Lett. 38 (2013) 4888–4891.
[10] M. Dong, K. Goyal, B. Worth, S. Makkar, W. Calhoun, L. Bali, S. Bali, Accurate in situ measurement of complex refractive index and particle size in intralipid emulsions, J. Biomed. Opt. 18 (2013) 087003.
[11] S. Lofas, M. Malmqvist, I. Ronnberg, E. Stenherg, B. Liedherg, I. Lundstrom, Bioanalysis with surface plasmon resonance, Sensors Actuators B 5 (1991) 79–84.
[12] J. Frew, H. Hill, Direct and indirect electron transfer between electrodes and redox proteins, Eur. J. Biochem. 172 (1988) 261–269.
[13] S. Bent, Organic functionalization of group IV semiconductor surfaces: principles, examples, applications, and prospects, Surf. Sci. 500 (1) (2002) 879–903.
[14] B. Branch, M. Dubey, A.S. Anderson, K. Artyushkova, J.K. Baldwin, D. Petsev, A.M. Dattelbaum, Investigating phosphonate monolayer stability on ALD oxide surfaces, Appl. Surf. Sci. 288 (2014) 98–108.
[15] T. Soejima, S. Oshiro, Y. Nakatsuji, S. Ito, Dense aqueous colloidal gold nanoparticles prepared from highly concentrated precursor solution, J. Colloid Interface Sci. 362 (2011) 325–329.
[16] P.C. Lee, D. Meisel, Adsorption and surface-enhanced Raman of dyes on silver and gold sols, J. Phys. Chem. 86 (17) (1982) 3391–3395.
[17] W. Calhoun, H. Maeta, A. Combs, L. Bali, S. Bali, Measurement of refractive index of highly turbid media, Opt. Lett. 35 (2010) 1224–1226.
[18] W. Calhoun, H. Maeta, A. Combs, L. Bali, S. Bali, Reply to comment on "measurement of refractive index of highly turbid media", Opt. Lett. 36 (2011) 3172.
[19] M. McClimans, C. LaPlante, D. Bonner, S. Bali, Real-time differential refractometry without interferometry at a sensitivity level of 10^{-6}, Appl. Opt. 45 (2006) 6477–6486.
[20] See Supplementary information Sec. S-II for our cover slip cleaning method. On the other hand, with silver nanoparticles, we did not encounter any problem in cleaning the prism between sample-changes, indicating that a coverslip may not be necessary for silver colloids.
[21] See, for example, Equation 2 in Ref. [8].
[22] Aqueous suspensions of MPA-functionalized AuNPs are stable and at first glance seem to show no settling over the time frame of our experiments (~24 hrs). However, note that some mild settling occurs even in the case of unaggregated samples. This explains the difference in unaggregated α-values in Fig. 3 between our TIR sensor and the UV–Vis spectrophotometer.
[23] To convert UV–Vis absorbance to attenuation coefficient α, we multiply absorbance by $ln10$ and divide by the sample length of 1 cm.
[24] See R. N. M. Ducay, Direct detection of aggregates in turbid colloidal suspensions, Master's thesis (Miami University, Oxford OH, USA, 2015) for a more accurate description of the DLS results in Ref. [8].
[25] T. Zheng, S. Bott, Q. Huo, Techniques for accurate sizing of gold nanoparticles using dynamic light scattering with particular application to chemical and biological sensing based on aggregate formation, ACS Appl. Mater. Interfaces (2016) (Article in Press) 10.1021/acsami.6b06903.